Theor Chim Acta (1994) 89: 33–57

Theoretica
Chimica Acta

Valence bond corrected single reference coupled cluster approach

II. Application to PPP model systems

J. Planelles*, J. Paldus, X. Li*****

Department of Applied Mathematics, University of Waterloo, Waterloo, Ontario, N2L 3G1 Canada.
Fax: (519) 746–4319

Received September 28, 1993 / Accepted March 2, 1994

Summary. The recently proposed valence bond (VB) corrected single reference (SR) coupled cluster method with singly and doubly excited cluster components (CCSD) [Paldus and Planelles, Theor Chim Acta 89, 13–31 (1994)] is tested using a number of simple yet typical Pariser–Parr–Pople (PPP) π-electron model systems, including both cyclic and linear polyenes. The cluster analysis of various approximate VB wave functions, obtained with the PPP-VB approach [Li and Paldus, J Mol Struct (Theochem) 229, 249 (1991)], is carried out and the resulting three- and four-body connected cluster components are employed in the VB corrected CCSD method. The cluster structure and the correlation energies obtained are compared to full configuration interaction (FCI) or full VB (FVB) results, representing the exact solutions for these models, and the performance and potential of the CCSD-VB approach are discussed.

Key words: Coupled cluster method – Valence bond (VB) wave functions – VB corrected CCSD method – Cluster analysis – Correlation effects – PPP Hamiltonian

1 Introduction

Single reference (SR) coupled cluster (CC) approaches, truncated at the pair-cluster level (CCSD) [1, 2], represent an often employed size-extensive formalism providing a reliable description of correlation effects in nondegenerate ground states of small and medium size molecular systems (see, e.g., [2a, 3]). These desirable properties of the CCSD method result from the negligibility of connected 3- and 4-body clusters that generally characterize nondegenerate situations. However,

---

* *Permanent address*: Departament de Ciències Experimentals, Campus de la Carretera de Borriol, Universitat Jaume I, Apartat 224, 12080 Castelló de la Plana, Spain

** Also at the Department of Chemistry and Guelph–Waterloo Center for Graduate Work in Chemistry, Waterloo Campus, University of Waterloo, Waterloo, Ontario, N2L 3G1, Canada

*** *Permanent address*: Department of Chemistry, Xiamen University, Xiamen, Fujian, China once the reference configuration becomes quasidegenerate with one or more excited configurations (as invariably is the case for nonequilibrium nuclear conformations that one must consider when dissociating or forming one or more chemical bonds, or when exploring an entire potential energy surface), the negligibility of higher than 2-body connected cluster components no longer holds. In such cases, the CCSD description steadily deteriorates with increasing quasidegeneracy and may even break down completely (in the sense that no real energy solution exists). Such situations are well documented in the literature [2, 4–6]. For very accurate calculations, 3-body clusters should be accounted for even when no quasidegeneracy is present (cf. [3]).

At the same time, it is well known that the energy is completely determined by one- and two-body cluster components, as long as the Hamiltonian considered involves at most two-body interactions. Nonetheless, the chain of CC (or, similarly, CI) equations is completely coupled in the sense that the equations determining the i-body clusters are coupled with those involving $(i-2)$, $(i-1)$, $(i+1)$ and $(i+2)$-body clusters. Consequently, we require the 3- and 4-body clusters to be negligible in order to truncate the chain of CC equations at the pair-cluster level, since the coupling terms involving these clusters may then be safely neglected. Were we able to obtain a reasonable estimate of these 3- and 4-body clusters from some independent source, however, the same truncation could be achieved even in quasidegenerate cases. This is precisely the idea behind the VB corrected CCSD approach, in which we employ an approximate VB wave function to determine the 3- and 4-body connected cluster components, that are then used to decouple the CC chain of equations. We outlined this approach in greater detail in Part I of this series [7] and will refer to it in the following as the CCSD-VB method.

More precisely, employing the standard SR CC Ansatz for the exact wave function

$$|\Psi\rangle=\exp(T)|\Phi_0\rangle, \quad T=\sum_{i=1}^{N} T_i, \tag{1}$$

the mono- and bi-excited subsets of the CC chain of equations take the form [1, 2, 7]

$$\langle \Phi_{J_1}^{(1)}|H_N(1+T_1+T_2+\tfrac{1}{2}T_1^2+2T_1T_2+\tfrac{1}{6}T_1^3)|\Phi_0\rangle_C+\langle \Phi_{J_1}^{(1)}|H_NT_3|\Phi_0\rangle=0, \tag{2a}$$

$$\begin{aligned}&\langle \Phi_{J_2}^{(2)}|H_N(1+T_1+T_2+\tfrac{1}{2}T_1^2+\tfrac{1}{2}T_2^2+2T_1T_2+\tfrac{1}{2}T_1^2T_2+\tfrac{1}{6}T_1^3+\tfrac{1}{24}T_1^4|\Phi_0\rangle_C\\&\quad+\langle \Phi_{J_2}^{(2)}|H_N(T_3+T_4+T_1T_3)|\Phi_0\rangle_C=0,\end{aligned} \tag{2b}$$

where the subscript C implies that only connected terms contribute and H_N designates the normal product form (with respect to $|\Phi_0\rangle$) of the electronic Hamiltonian (see, e.g. [1, 2b]):

$$H_N=H-\langle \Phi_0|H|\Phi_0\rangle=F_N+V_N, \tag{3a}$$

$$F_N=\sum_{i,j}\langle i|\hat{f}|j\rangle\sum_{\sigma}n[X_{i\sigma}^{\dagger}X_{j\sigma}], \tag{3b}$$

$$V_N=\tfrac{1}{2}\sum_{i,j,k,l}\langle ij|\hat{v}|kl\rangle\sum_{\sigma,\tau}n[X_{i\sigma}^{\dagger}X_{j\tau}^{\dagger}X_{l\tau}X_{k\sigma}], \tag{3c}$$

with

$$\langle i|\hat{f}|j\rangle = \langle i|\hat{z}|j\rangle + \sum_{\substack{a \\ (\text{occupied})}} (2\langle ia|\hat{v}|ja\rangle - \langle ia|\hat{v}|aj\rangle). \tag{3d}$$

Here we designate the annihilation (creation) operator of the second quantization formalism that is associated with the spinorbital $|i\rangle|\sigma\rangle \equiv |I\rangle$ as $X_{i\sigma}(X_{i\sigma}^{\dagger})$, while using Dirac notation for two-electron integrals $\langle ij|\hat{v}|kl\rangle \equiv \langle i(1)j(2)|\hat{v}|k(1)l(2)\rangle$. Finally, $|\Phi_{J_n}^{(n)}\rangle$ designates the n-times excited configuration [defined by the appropriate set of occupied and virtual (spin) orbital labels and, in the spin-adapted formalism, also by appropriate intermediate spin coupling quantum numbers] relative to the reference $|\Phi_0\rangle$.

Thus, neglecting the T_3 and T_4 components, i.e., by setting $T_3 = T_4 = 0$, we obtain the well known CCSD equations (or their variants resulting by neglecting small higher order contributions, such as those represented by cubic and quartic terms) that we can write in the general form

$$a_i + b_{ij}t_j + c_{ijk}t_jt_k + \cdots = 0, \tag{4}$$

where the summation convention over repeated indices is implied and where we assume some arbitrary but fixed labeling of mono- and bi-excited configurations. Assuming now that we can find some independent estimate of the T_3 and T_4 cluster components, we can evaluate the corresponding terms involving these clusters [the second term on the left-hand side of Eqs. (2)], and correct accordingly the absolute and linear terms in Eq. (4), thus obtaining the *corrected* CCSD equations

$$a_i' + b_{ij}'t_j + c_{ijk}t_jt_k + \cdots = 0. \tag{5}$$

Employing a VB wave function as the source of 3- and 4-body components, we thus arrive at the CCSD-VB method. The explicit form of the required corrections was given in Part I. We recall that for simplicity sake, we also employ approximate 1-body components of T_1 in order to correct for the presence of T_1T_3 clusters through absolute rather than linear terms. For details, we refer the reader to Part I.

Prior to working out various technical problems and generating appropriate codes at the *ab initio* level, we consider it worthwhile to test this idea on simple semiempirical model systems, in particular those described by the Pariser–Parr–Pople (PPP)-type Hamiltonians [8, 9]. This choice has several advantages that we list below.

(a) PPP π-electron models enable us to explore the broad regime of correlation effects by simply changing the appropriate coupling constant, which may be conveniently chosen as the reciprocal value of the resonance integral β. Thus, scaling the resonance integral β for a given system, while keeping the two-electron Coulomb integrals fixed, we can examine the correlation effects from the fully correlated limit ($\beta = 0$) to a completely noncorrelated limit (in practice, $\beta \sim -5$ eV), in which the Hückel approximation becomes exact and the correlation energy tends to zero.

(b) For sufficiently small model systems we can easily obtain the exact solution using either the full configuration interaction (FCI) [10] or full valence bond (FVB) [11, 12] codes. This will in turn enable us to make a direct comparison of approximate and exact cluster amplitudes and to explore separately the role of various correction terms involving T_3, T_4 and T_1T_3 clusters.

(c) The easy accessibility of exact solutions also facilitates testing our codes, since by employing exact 3- and 4-body cluster amplitudes we must obtain exact FCI energies when solving the CCSD-VB equations.

(d) Finally, we can also exploit these models to simulate bond breaking or formation when we use "Mulliken's magic formula" [13, 14] for the resonance integrals and proceed beyond the tight binding approximation at the one-electron level. Such models will be employed in Part III of this series [15].

In the next section we briefly characterize the models and methods employed, while in Sects. 3 and 4 we present results for cyclic and linear polyenic systems, respectively. In the last section we discuss these results and draw appropriate conclusions.

2 Models and method employed

We consider various homonuclear π-electron model systems as described by the PPP Hamiltonian of the form [9]

$$H_\pi = \beta \sum_{\mu,\nu}{}' E_{\mu\nu} + \tfrac{1}{2} \sum_{\mu,\nu} \gamma_{\mu\nu}(n_\mu - 1)(n_\nu - 1), \tag{6}$$

where

$$E_{\mu\nu} = \sum_\sigma X^\dagger_{\mu\sigma} X_{\nu\sigma} \tag{7}$$

are the atomic orbital unitary group generators [9] and $n_\mu = E_{\mu\mu}$ is the μth site occupation number operator. The one-electron resonance integral β, $\beta = \langle \mu | \hat{z} | \nu \rangle$ with μ and ν being nearest neighbors, can be employed as a coupling constant (or, rather, its reciprocal value β^{-1}) which measures the magnitude of correlation effects. It is thus instructive, at least for certain archtypal systems, to explore the whole range of correlation effects (by scaling the resonance integral β) from a weakly correlated regime ($\beta \sim -5$ to -10 eV), where correlation effects are negligible, to the fully correlated limit ($\beta = 0$), where the correlation effects predominate and where many standard approaches to the correlation problem break down. The two-electron part of the PPP Hamiltonian contains only Coulomb-type integrals $\gamma_{\mu\nu} = e^2 \langle \mu\nu | r_{12}^{-1} | \mu\nu \rangle$ thanks to the zero differential overlap (ZDO) approximation employed [8]. The one-center integral γ_{00} is given by the difference between the valence state ionization potential and electron affinity of the sp^2 hybridized carbon atom [8]. We shall employ the value of $\gamma_{00} = 10.840$ eV. For the 2-center Coulomb integrals we then use the Mataga–Nishimoto approximation [16]

$$\gamma_{\mu\nu} = e^2/(R_{\mu\nu} + a), \quad a = e^2/\gamma_{00}. \tag{8}$$

Finally, the prime on the first summation symbol in Eq. (6) indicates that we employ the tight binding approximation for the one-electron part, so that the sum extends over nearest neighbors only.

In order to obtain meaningful VB wave functions, involving only a few covalent structures, it is essential to employ the so-called overlap enhanced atomic orbitals (OEAOs) [17, 18]. In contrast to the orthonormal AO's χ_μ of the PPP model, $\langle \chi_\mu | \chi_\nu \rangle = \delta_{\mu\nu}$, each localized on the atomic site μ, the OEAOs are nonorthogonal, suitably delocalized atomic orbitals that provide an optimal bonding within the VB scheme considered. Ideally one assumes the LCAO form for the OEAOs (as in the MO calculations) without, however, enforcing the orthogonality, and uses the variation principle to determine the optimal values of these LCAO coefficients once the desirable form of the VB wave function is chosen [say, all covalent structures or some appropriate subset of the latter, e.g., all Kekulé type structures, etc.]. We have shown earlier [11, 19, 20] that for the PPP models it is sufficient to consider at most two variational parameters. In the simplest one-parameter case, the unnormalized OEAOs have the form

$$\phi_\mu^{(1)}=\chi_\mu+\varepsilon_1 \sum_{\substack{\nu \\ (\nu\neq\mu)}}^{(1)} \chi_\nu, \tag{9}$$

with the summation extending over nearest neighbors of μ, and χ_τ designating an orthonormal PPP AO on site τ. In general, multi-parameter OEAOs can be chosen with, say, one-parameter (ε_1) associated with nearest neighbors, a second parameter (ε_2) with next nearest neighbors, etc. For honeycomb lattices of aromatic systems it also makes sense to choose ε_3 as the second parameter, i.e., to set $\varepsilon_2=0$ (for meta positions), namely to admix to a given χ_μ only its nearest and second next neighboring χ_τ's (i.e., from ortho and para positions). Thus, when we shall employ 2-parameter OEAOs in the benzene case, they will be parametrized precisely in this way (i.e., $\{b1, 3\}$ basis of [11]).

The computational algorithm that was developed for the PPP-VB method exploits the formalism of the Clifford algebra unitary group approach (CAUGA) [21, 22] and was described in detail elsewhere [12]. Briefly, the spin-free Rumer–Weyl VB basis vectors [21d] are labeled by bonded tableaux [23] and are expressed in terms of bi-spinor CAUGA states. The latter can be put into a one to one correspondence with the Waller–Hartree bi-determinantal states [24]. Note that the action of $U(N)$ generators, $E_{\mu\nu}$, Eq. (7), which are defined in terms of orthogonal PPP AO's χ_μ, on the nonorthogonal OEAO basis $\{\phi_\mu\}$ is very simple. Writing, generally,

$$\phi_\mu=\sum_\nu \varepsilon_{\nu\mu}\chi_\nu, \tag{10}$$

we have that

$$E_{\mu\nu}\phi_\tau=\varepsilon_{\nu\tau}\chi_\mu. \tag{11}$$

Thus, acting with the PPP Hamiltonian (6) on our VB states and calculating the overlap with the resulting states, we obtain a standard variational eigenvalue problem of the non-orthogonal type

$$\boldsymbol{HC}=\boldsymbol{ESC}\,, \tag{12}$$

which is handled in a standard way (depending on the size of the problem).

The available PPP-VB programs [11, 12] are capable of exploiting an arbitrary set of covalent and/or ionic VB structures, including the full VB (FVB). Clearly, the latter is identical with the corresponding FCI, in which case we can directly exploit the orthogonal PPP basis, avoiding nonorthogonality problems. It is also clear that OEAO basis is undefined in the FVB case, since any basis set will yield the same resulting FCI energy. We may thus expect that it may become difficult to determine the OEAO basis when very large VB expansion (close to FVB) would be employed. However, the whole idea of VB approaches is to employ only a few structures in the VB expansion, in which case the search for the optimal OEAOs creates no problems.

For all the systems considered in this paper we employ approximate VB wave functions involving only covalent-type structures: we either employ all Kekulé type structures or all covalent structures. As already mentioned, our PPP-VB studies [11, 12, 19, 20] of various π-electron systems (both alternant and nonalternant; aromatic, nonaromatic and antiaromatic; neutral, ionic, radicaloid or biradicaloid species), revealed that a one-parameter description provides very satisfactory results. Moreover, when employing the standard spectroscopic parameterization ($\beta \sim -2.4$ eV), the value of the mixing parameter ε_1, Eq. (9), changes very little from one system to another, so that when using its average value $\varepsilon_1^{(ave)} = 0.31$, only very small changes in the calculated π-electron energies result [11, 12, 19, 20]. Thus, for all practical purposes, the simplest PPP-VB method exploiting the nearest neighbor OEAO basis with fixed mixing parameter $\varepsilon_1 = \varepsilon_1^{(ave)} = 0.31$ and only covalent (or even only Kekulé) structures, provides a very good description of the studied models [11, 12, 19, 20].

Nonetheless, when we wish to explore the whole range of the coupling constant, we cannot avoid the optimization step determining the mixing parameter(s) ε_1 (or ε_1 and ε_3), since they change rapidly with β. Thus, as long as we carry out studies for different correlation regimes by varying the resonance integral β, we always optimize mixing parameter(s).

Once a suitable PPP-VB wave function is determined, we then carry out a standard cluster analysis and from the resulting 3- and 4-body (and 1-body in case of $T_1 T_3$ correction) cluster amplitudes, expressed relative to the standard SCF MO (or HF) basis, we calculate corrections to the absolute terms of the CCSD equations. Having these corrections, we finally carry out the standard CCSD calculations. All these steps were described in considerable detail in Part I, where we also presented an explicit form of all the required correction terms.

The choice of our model systems that are considered below was guided by the following considerations. We first start with regular cyclic polyenes, which were carefully studied earlier using various methods (see, e.g., [5, 6, 14]). In view of the high spatial symmetry of these models, the standard Hückel MOs are simultaneously the HF or SCF MOs as well as Brueckner (or maximum overlap) MOs. Consequently, the T_1 cluster component exactly vanishes in this case. Moreover, when considering the 4-membered ring, representing the PPP model of cyclobutadiene, even the T_3 clusters vanish in view of the particle–hole symmetry. Thus, in this simplest case, only one T_4 cluster component is involved, so that a detailed study can be accomplished. We thus start our investigations with this simplest system, followed by two aromatic-type cyclic polyenes (with non-degenerate ground state), namely C_6H_6 and $C_{10}H_{10}$, the first one representing the PPP model of benzene. Thus, both archtypal antiaromatic (C_4H_4) and aromatic (C_6H_6) systems are included. We then explore linear polyenes as representatives of nonaromatic systems, namely *trans*-butadiene and all-*trans*-hexatriene, where all cluster components (T_1, T_3 and T_4) have nonvanishing components.

3 Results and discussion

In order to present succinctly our results, we introduce a shorthand notation that describes the CCSD-VB method employed. We designate the number of Kekulé (K) or covalent (c) structures and the number of mixing parameters (ε) involved in the VB wave function, providing the cluster components which were used to evaluate the correcting terms (T_1, T_3 and/or $T_1 T_3$), as follows: CCSD-VB(nK, $m\varepsilon$)

Table 1. Comparison of the exact (FCI) and approximate [PPP-VB($2K$, 1ε)] t_4-amplitudes for the π-electron model of cyclobutadiene as a function of the resonance integral β (in eV). R designates the ratio of VB and FCI amplitudes, $R = t_4^{\text{PPP-VB}}/t_4^{\text{FCI}}$. Optimal values of the mixing parameter ε_1, Eq. (9), characterizing the OEAO $\{b1\}$ basis employed in the VB model, are also given

$-\beta$ (eV)	ε_1	t_4		R
		VB($2K$, 1ε)	FCI	
0.25	0.0443	−0.46721	−0.46954	0.99505
0.5	0.0847	−0.33624	−0.34096	0.98615
1.0	0.1490	−0.19499	−0.20068	0.97162
1.5	0.1947	−0.12872	−0.13249	0.97160
2.0	0.2289	−0.09218	−0.09432	0.97733
2.5	0.2553	−0.06996	−0.07069	0.98977
3.0	0.2774	−0.05463	−0.05499	0.99341
3.5	0.2948	−0.04444	−0.04401	1.00978
4.0	0.3102	−0.03657	−0.03603	1.01488
5.0	0.3345	−0.02624	−0.02543	1.03187
10.0	0.4001	−0.00821	−0.00784	1.04628

implies that n Kekulé structure wave function built from m-parameter OEAOs was employed, and similarly CCSD-VB(nc, $m\varepsilon$) indicates that also non-Kekulé covalent structures were employed. When only certain correcting terms are considered, this is indicated by corresponding abbreviations T_3, T_4 and T_1T_3.

3.1 Cyclic polyenes

3.1.1 Cyclobutadiene. Considering the PPP model of C_4H_4, we assume the C–C bond length to be 1.4 Å with carbon nuclei forming a regular square. We also employ the tight binding approximation for the one-electron part (see Part III [15] for models going beyond this approximation). As already mentioned, both T_1 and T_3 clusters vanish, while T_4 involves a single cluster component $t_4 \equiv \langle 3344|\hat{t}_4|1122\rangle$. Thus, in this case CCD ≡ CCSD ≡ CCSDT.

Considering a VB wave function involving two Kekulé structures (which in this simple case is equivalent to an all covalent structure wave function), we optimized mixing parameter ε_1 to minimize the energy and subsequently cluster analyzed the resulting wave function. The results are summarized in Table 1, where the t_4 cluster component arising from the two Kekulé structure VB wave function is compared with the exact result obtained by cluster analyzing the FCI wave function. We find that in the whole region of β values, the t_4 component resulting from the approximate VB wave function (2 Kekulé structures) provides an excellent approximation. Since each Kekulé structure wave function represents an exact solution in the fully correlated $\beta = 0$ limit [as the form of the PPP Hamiltonian given by Eq. (6) immediately implies], the best approximation is obtained for small $|\beta|$ values, and it deteriorates as $|\beta|$ increases until $\beta = -1.5$ eV. It then starts again improving until $\beta \sim -3.5$ eV when it again starts deteriorating with further increase in $|\beta|$ (see Table 1). However, even for very large $|\beta|$ values ($\beta = -10$ eV), the error in t_4 does not exceed 5%. Since, at the same time, the magnitude of the t_4 amplitude decreases

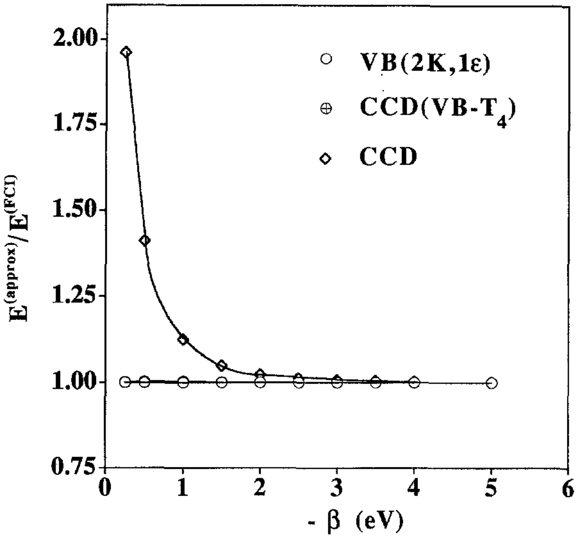

Fig. 1. Relative correlation energies $E^{(approx)}/E^{(FCI)}$ obtained with the PPP-VB($2K$, 1ε) approximation (○) and with the standard (◇) and VB corrected (⊕) CCSD approaches as a function of the resonance integral β (in eV) for the π-electron model of cyclobutadiene. Note that within the scale of the figure, the PPP-VB($2K$, 1ε) and CCD-VB energies coincide, both being almost identical with the FCI energy (cf. also Table 1)

with increasing $|\beta|$, and correspondingly its effect on the correlation energy (in fact the correlation energy itself approaches 0 as $|\beta|\to\infty$), this inaccuracy in t_4 should have little effect. Let us also mention that even the pair clusters resulting from the 2 Kekulé VB wave function are very close to the exact pair cluster amplitudes in the whole range of the coupling constant examined ($0 \leqslant |\beta| \leqslant 10$ eV).

As might be expected, we obtain very good correlation energies when employing the VB corrected CCSD procedure. Indeed, while the standard CCD steadily deteriorates when approaching the fully correlated limit (and in fact breaks down completely for very small $|\beta|$ values), the CCD-VB ($2K$, 1ε) provides a practically exact result for all coupling constants considered as Fig. 1 indicates.

It is also of interest to examine how critical is the optimization of mixing parameter ε_1 for the performance of the CCSD-VB procedure or, equivalently, for obtaining of reasonably accurate t_4 cluster components. We recall that when employing an average value for the mixing parameter when applying the PPP-VB procedure with spectroscopic parameterization, we still obtain perfectly acceptable approximation. We thus consider the cyclobutadiene model with $\beta = -2.5$ eV and vary the mixing parameter in the vicinity of its optimal value. For the sake of comparison, we also calculate the corresponding PPP-VB energies using the same 2-Kekulé structure wave function that we employed to obtain the CCSD correction terms. The ratio of the resulting CCSD-VB and PPP-VB energies with respect to the exact result is shown in Fig. 2, while the ratio of the corresponding t_4 amplitudes is listed in Table 2. We see immediately from Fig. 2 that the VB energy is much more sensitive to the change in the mixing parameter than is the CCD-VB energy, the former showing a parabolic dependence with the maximum corresponding to the optimal ε_1 value while the latter one depends nearly linearly on ε_1. This would seem to indicate that a very accurate optimization of the mixing parameter is not essential, even though the t_4 amplitudes change by a factor of 2 to 3 as Table 2 indicates. We also note that the optimal ε_1 value that results from the VB energy minimization is not giving the "best" CCD-VB energy. However, the

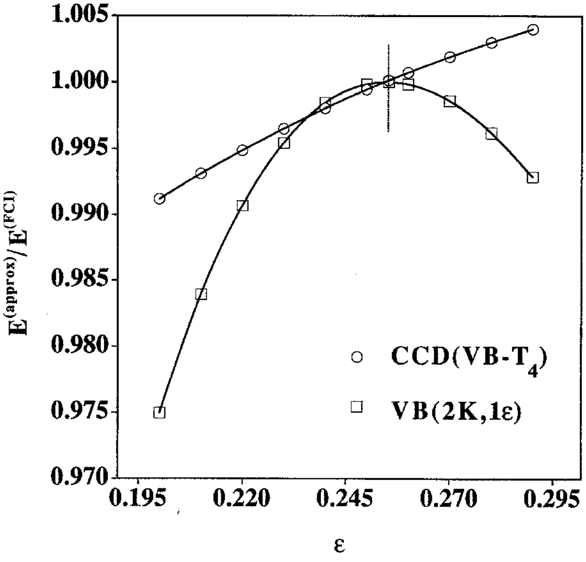

Fig. 2. The effect of the mixing parameter ε_1, Eq. (9), defining the OEAO $\{b1\}$ basis used in the 2 Kekulé structure PPP-VB model of cyclobutadiene, on the PPP-VB and CCSD-VB energies. The spectroscopic parameterization ($\beta=-2.5$ eV) is employed yielding the FCI correlation energy -6.7745 eV. The vertical line indicates the optimal value of ε_1 corresponding to $\beta=-2.5$ eV

Table 2. Dependence of the t_4 amplitude of cyclobutadiene, obtained from the PPP-VB(2K, 1ε) wave function for $\beta=-2.5$ eV, as a function of the mixing parameter ε_1, Eq. (9), defining the OEAO $\{b1\}$ basis employed. Relative values R of the ratio of the PPP-VB and FCI amplitudes, $R=t_4^{\text{PPP-VB}}/t_4^{\text{FCI}}$, are given. The ε_1 independent FCI amplitude equals in this case $t_4^{\text{FCI}}=-0.070688$. The optimal value of ε_1 corresponding to $\beta=-2.5$ eV is $\varepsilon_1=0.255313$

ε_1	R
0.20	1.7323
0.21	1.5734
0.22	1.4263
0.23	1.2902
0.24	1.1643
0.25	1.0479
0.255313	0.9898
0.26	0.9405
0.27	0.8415
0.28	0.7503
0.29	0.6664

ε_1 parameter value, which yields the exact FCI energy with the CCD-VB procedure, lies in the close vicinity of the optimal VB parameter.

3.1.2 Benzene. We next consider a prototypical aromatic system represented by the PPP model of benzene. We again assume the C–C bond length to be 1.4 Å, with

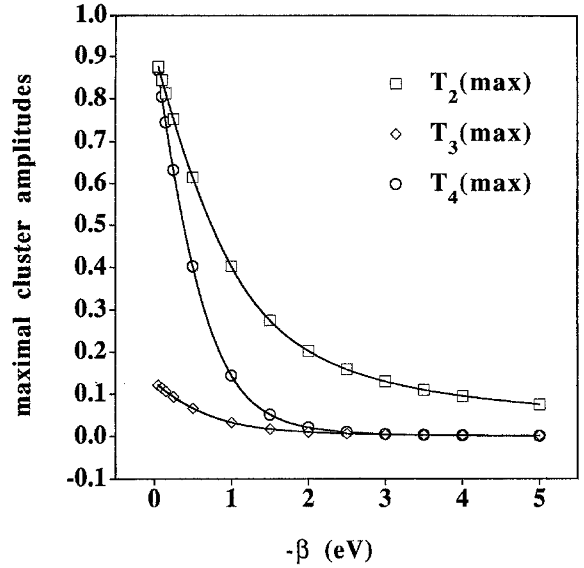

Fig. 3. Dependence of the exact FCI maximal t_2, t_3 and t_4 cluster amplitudes of the π-electron benzene model on the resonance integral β (in eV)

carbons located at the vertices of a regular hexagon and assume the tight binding approximation for the one-electron part. Although in this case both T_3 and T_4 clusters contribute, we still have that $T_1 = 0$. Thus, again CCD ≡ CCSD and only T_3 and T_4 corrections need be considered.

Before exploring the CCD-VB approach, let us examine the cluster structure and energetics of the exact FCI or FVB solution. Since in this case we have to deal with a number of cluster amplitudes of T_2, T_3 and T_4 types, we cannot examine them individually. In order to get a general idea of their relative importance, we have plotted in Fig. 3 the maximum absolute value of a cluster amplitude from each class as a function of the resonance integral β. A similar dependence is obtained when we examine the sum of the squares of cluster amplitudes of each kind. Later, we also present another insight into the cluster structure using a nomogrammatic representation.

We can see clearly from Fig. 3 that for $|\beta| > |\beta^{(\mathrm{spect})}|$, where the spectroscopic or physical value of β is in the neighborhood of −2.4 eV, both 3- and 4-body connected clusters are very small while their significance dramatically increases when approaching the fully correlated limit. We shall also see that t_3 amplitudes, although much smaller than t_4-amplitudes, play an important role in the region of high coupling constants. Moreover, their effect on the correlation energy is far from being additive. To demonstrate this fact, as well as to get some idea concerning the role of 3- and 4-body clusters, we have carried out the CCD-VB calculations using the FCI amplitudes and applied the T_3 and T_4 corrections separately as well as jointly. Of course, in this case, the CCD-VB method considering all three corrections must yield the FCI energy. These results are shown in Fig. 4. We find that for $|\beta| > 2$ eV, the contribution from 3- and 4-body clusters is very small, so that the VB corrected CCD energies are practically identical with the standard CCD ones, both providing an excellent approximation to the exact FCI results. As we approach the fully correlated limit (i.e. for $|\beta| < 2$ eV), however, the standard CCD energy begins to significantly overestimate the exact correlation energy. Applying

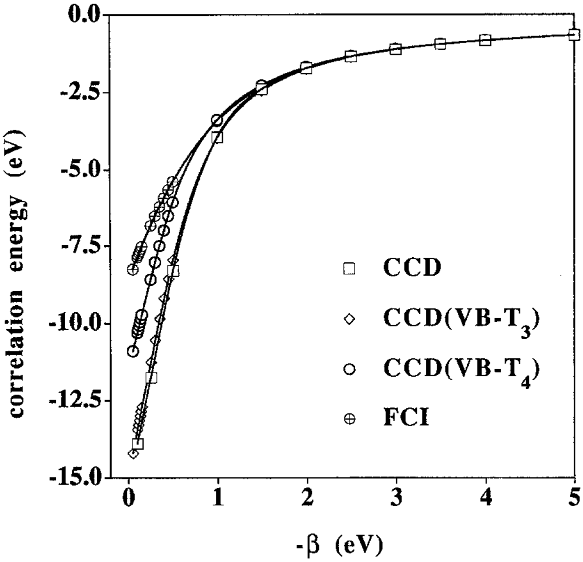

Fig. 4. Comparison of correlation energies (in eV) of the benzene π-electron model, obtained with the FCI and different CCD methods, as a function of the resonance integral β (in eV). Note that in this case, CCD ≡ CCSD. In addition to the standard CCD model, both T_3 and T_4 corrected CCD-VB models, employing, respectively, exact 3- and 4-body connected cluster amplitudes, are shown. Note that in this case the T_3 *and* T_4 corrected CCD-VB is equivalent to FCI

T_3 corrections, only a small change is observed, while T_4 corrections reduce the CCD error to about one half for $|\beta| < 0.5$ eV and almost completely for 1 eV $< |\beta| < 2$ eV. We thus see that in the highly correlated regime, the effect of the T_3 and T_4 correcting terms is highly nonadditive, each providing much smaller correction individually than when both are applied simultaneously. It is also interesting that both corrections shift the CCD energy "in the right direction", i.e. improve the standard CCD result. This should be compared with *ab initio* model calculation on the H_4 models [25], where the T_3 and T_4 contributions shift the correlation energy in opposite directions (see, however, Part III).

Let us now investigate the performance of the CCD-VB method using approximate VB wave functions. We consider VB wave functions involving only two Kekulé structures, with one or two parameter OEAOs, as well as the one with all five covalent structures (Kekulé and Dewar) and one-parameter OEAO basis. The cluster analysis of these wave functions indicates that they provide a reasonable estimate of the connected 3- and 4-body clusters. This is illustrated in Figs. 5a and 5b, which compare the maximal t_3 and t_4 clusters obtained from various VB wave functions and in Figs. 6a–d and 7a–d, where the distribution of magnitudes of the t_3 and t_4 clusters for five different values of the resonance integral is represented by nomograms. These nomograms also clearly indicate how the importance of the 3- and 4-body clusters increases when approaching the fully correlated limit. The wave function containing both Kekulé and Dewar structures seems to provide the closest approximation to the FCI picture, although the results based only on Kekulé structures, particularly for the more important T_4 clusters, provide a rather good description as well.

The performance of the CCD-VB method, employing the above mentioned approximate VB wave functions, is shown in Figs. 8 and 9. We see from Fig. 8a that all three approximate VB wave functions successfully correct the shortcomings of the standard CCD method in the highly correlated regime. The details for this region are shown in Fig. 8b, where we also included several points obtained with

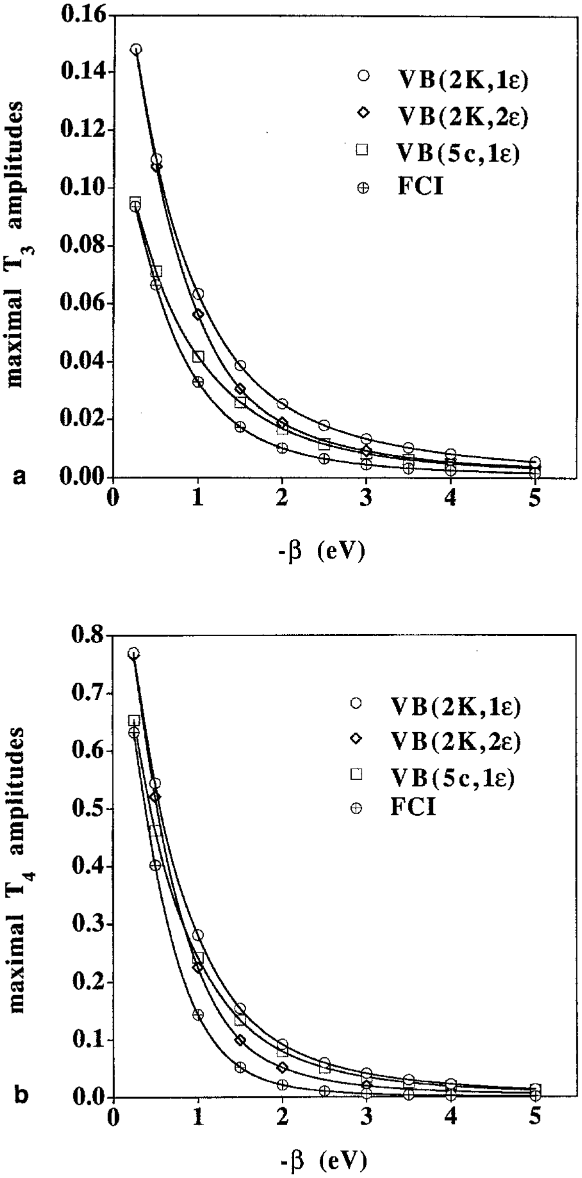

Fig. 5a, b. Comparison of maximal t_3 (**a**) and t_4 (**b**) amplitudes as a function of the resonance integral β (in eV) resulting from the FCI and different PPP-VB wave functions of the benzene π-electron model

the VB wave function involving 5 covalent structures and two-parameter $\{b1, 3\}$ OEAO basis. We see that in all cases the corrected CCD-VB correlation energies approach the exact value as $\beta \to 0$, as might be expected. It is, however, surprising that simple two-Kekulé structure wave functions yield slightly better energies than those involving all 5 covalent structures (clearly, the opposite is the case for the VB energies, that are variational). We also see that the introduction of the second mixing parameter in the OEAO basis has very little effect and leads to only a marginal improvement. Finally, in the neighborhood of physical

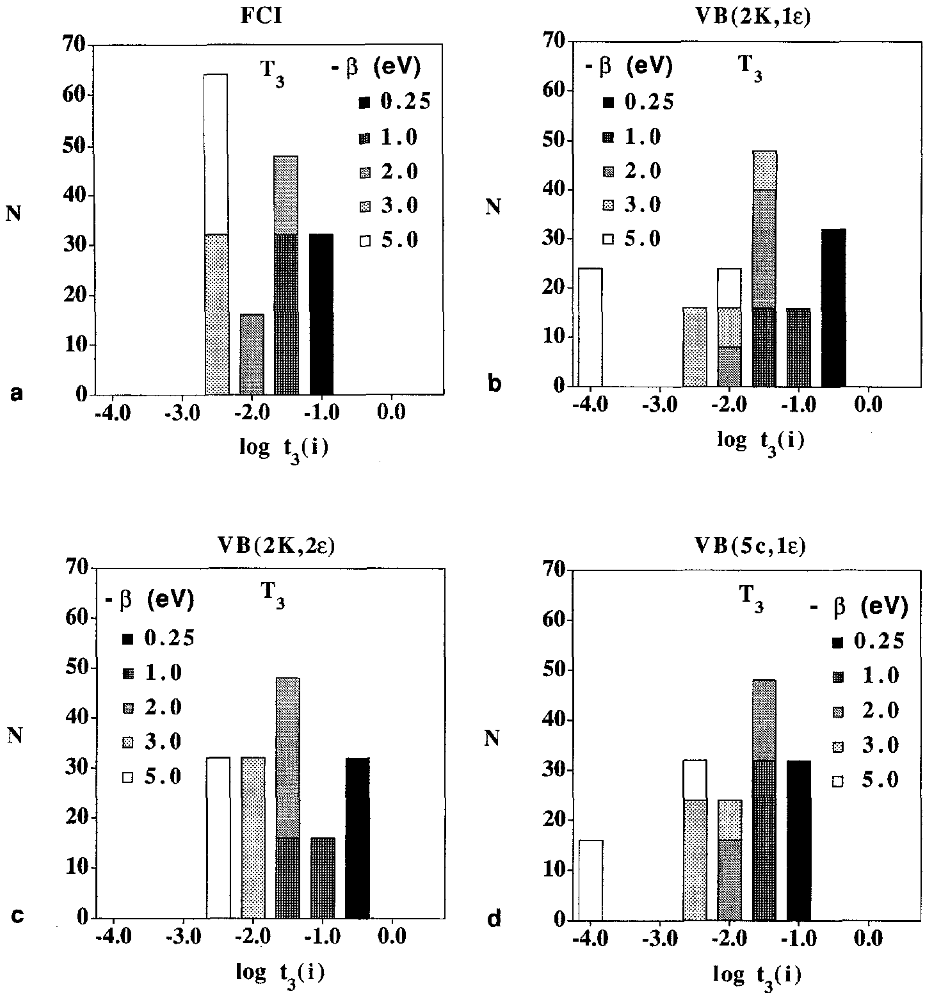

Fig. 6a–d. Comparison of the cluster structure of the FCI and three approximate VB wave functions for benzene. Each nomogram shows the number N of $|t_3|$ amplitudes, whose logarithm is in the indicated range, for 5 typical values of the resonance integral β. The amplitudes whose absolute value is smaller than 10^{-4} are all counted in the leftmost box

parameterization ($\beta = -2.4$ eV) and in the weakly correlated limit, the standard CCD provides an almost exact result and the T_3 and T_4 corrections have a negligible effect.

Figure 9 examines the role of the T_3 and T_4 corrections individually, relative to the FCI results. Again, we see that we obtain a very similar picture when either the 2 Kekulé or the 5 covalent structure VB wave function is employed. Initially, for $1\ \text{eV} < |\beta| < 3\ \text{eV}$, the T_3 and T_4 corrections deviate from the corresponding FCI corrections in opposite directions. However, for $|\beta| < 1$ eV, both differences E(CCD-VB)-E(FCI) become negative. Yet, when both considered simultaneously, a positive deviation results that tends to zero as $|\beta| \rightarrow 0$.

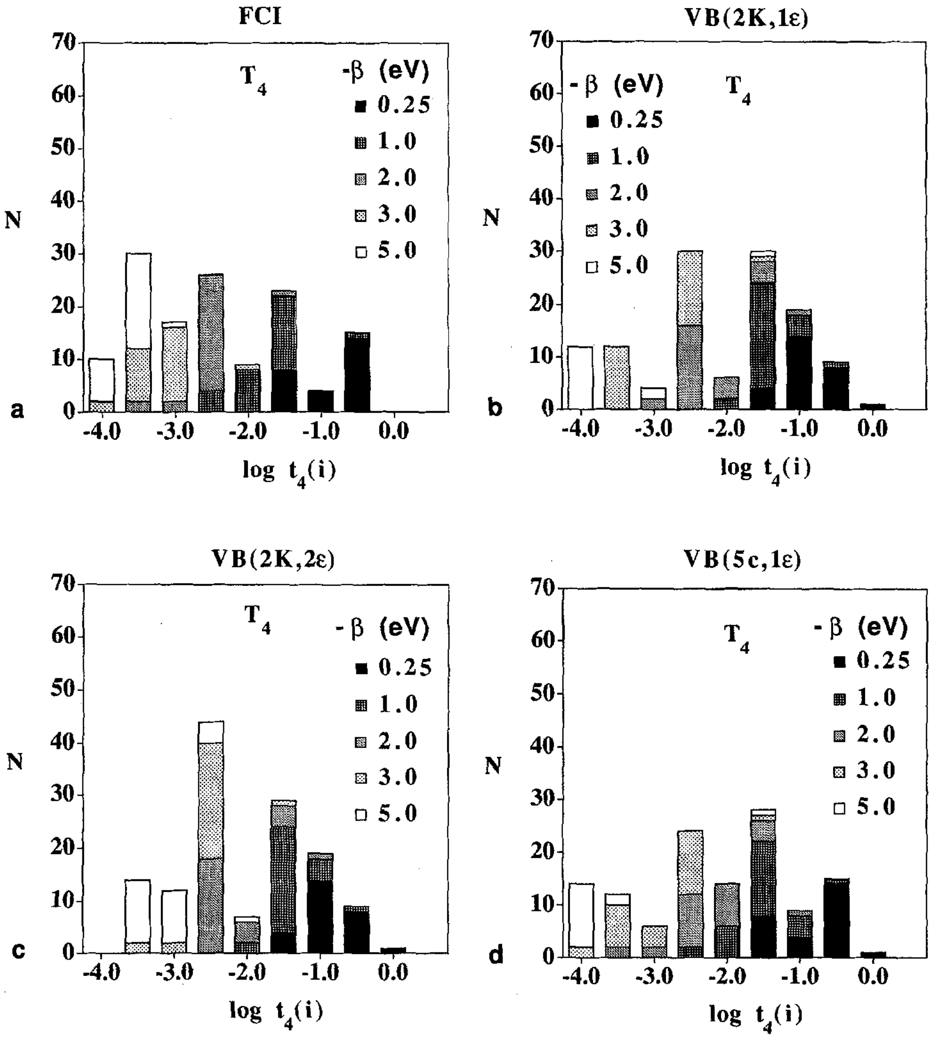

Fig. 7a–d. Same as Fig. 6 for the t_4 amplitudes

Here we must also emphasize that much care must be exercised when solving the CCD or CCD-VB equations in the highly correlated region. The standard CCD solution can only be continued beyond $\beta \sim -1$ eV using "analytic continuation" procedure, i.e. by employing the t_2 amplitudes for a nearby geometry as a starting approximation, or some other meaningful estimate of t_2 amplitudes. Similar difficulties occur for very small $|\beta|$ values when individual (i.e., T_3 or T_4) corrections are applied. The fully corrected CCD-VB equations converge best, although again in the highly correlated regime, a proper choice of the initial approximation is crucial for the Newton–Raphson iterative procedure to converge.

Thus, to conclude, we see that already a simple ($2K$, 1ε) VB wave function provides a reasonable estimate of the 3- and 4-body clusters and the corresponding CCD-VB method is capable of correcting major inadequacies of the standard CCD approach.

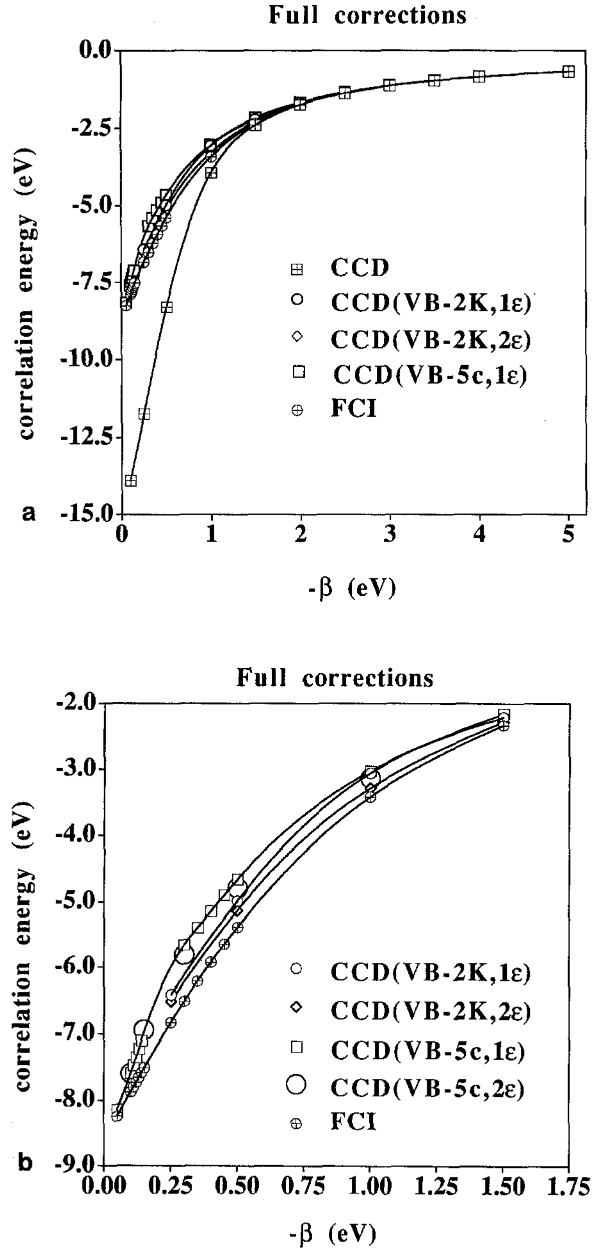

Fig. 8a, b. Dependence of the correlation energy (in eV) of the benzene π-electron model on the resonance integral β (in eV) obtained with the FCI, CCD and various VB corrected CCD methods. **b** highlights the highly correlated region

3.1.3 $C_{10}H_{10}$. We briefly next consider the $N=10$ cyclic polyene, using the same parametrization as in the benzene case, and the $(2K, 1\varepsilon)$ VB wave function. The main results are summarized in Fig. 10, where the PPP-VB energy is also shown. We recall that in this case, the CCD method gives extremely poor results for $|\beta| < 1$ eV (the error for $\beta = 0$ is about 1000%) [5], not to mention the difficulty of

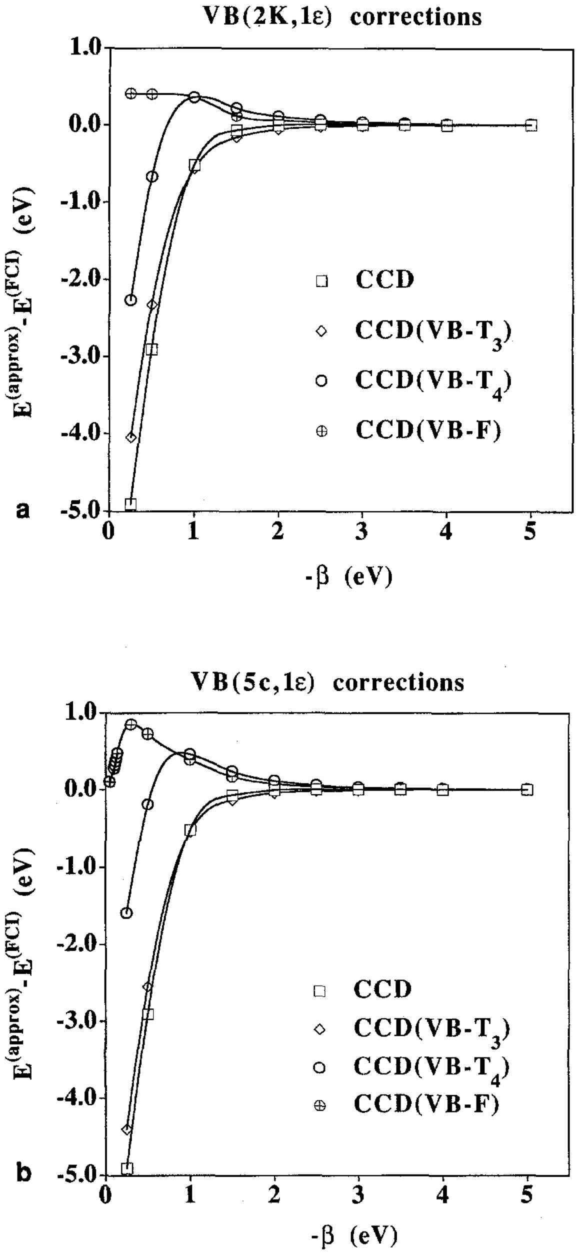

Fig. 9a, b. Difference between approximate and FCI correlation energies (in eV) of the benzene π-electron model as a function of the resonance integral β (in eV) obtained with the CCD and VB-corrected CCD methods. In the latter case, the energy difference between the T_3, T_4 and fully (F) (i.e., involving both T_3 *and* T_4) corrected CCD-VB and the FCI correlation energies is shown. The corrections were calculated using the PPP-VB wave functions involving 2 Kekulé (**a**) and 5 covalent (**b**) structures

reaching the convergence in this region. We thus restrict ourselves to the region of $|\beta| > 1$ eV. We see that again, for $|\beta| > 3$ eV, the T_3 and T_4 corrections are small and the standard CCD method performs well. It must be noted, however, that the 2-Kekulé structure VB description deteriorates in this region as the corresponding energy indicates. Nonetheless, since the T_3 and T_4 corrections are very small in this

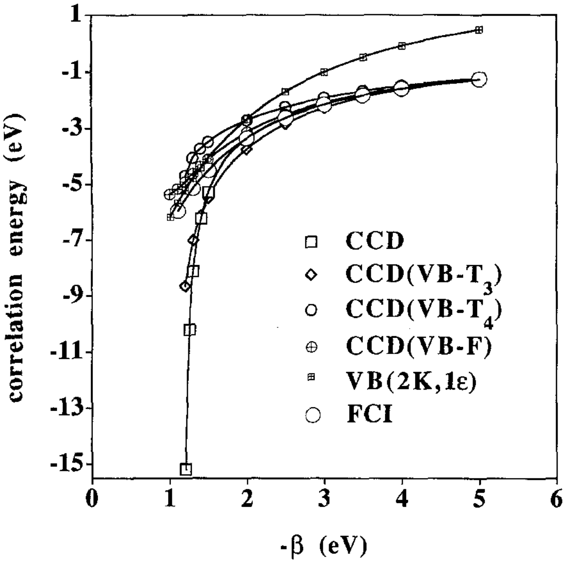

Fig. 10. Dependence of the correlation energy (in eV) of the $C_{10}H_{10}$ cyclic polyene as a function of the resonance integral obtained with the FCI, PPP-VB, CCD and various VB corrected CCD methods. T_3, T_4 and F labels imply the 3-body, 4-body and both 3- and 4-body corrections were applied

region, this has no adverse effect on the performance of the CCD-VB method that yields practically the same result in this region as the standard CCD.

For small $|\beta|$ values, we find behavior similar to the benzene case. The T_3 corrections by themselves have little effect, while the opposite is the case for the T_4 corrections. Nonetheless, to obtain a good approximation, it is essential to consider both corrections simultaneously (referred to as the full correction). We must also emphasize (see Fig. 10) the "complementarity" of VB and MO based descriptions, the former being well suited to the highly correlated limit and the latter one to the uncorrelated limit. Consequently, the CCD-VB approach provides a "bridge" between these two formalisms that performs rather well in the whole range of the coupling constant.

3.2 Linear polyenes

In both models examined here we assume all-trans conformation and idealized geometry with the C–C bond length of 1.4 Å and CCC angle of 120°. We again employ the tight binding approximation for the one-electron part and we note that for these models neither T_3, nor T_4, nor T_1 vanishes. We also invariably employ only one mixing parameter ε_1 in the OEAO bases in PPP–VB calculations. For the sake of reference, we list the exact FCI correlation energies for both systems in Table 3.

3.2.1 Trans-butadiene. Exploiting the simplicity of this 4-electron model problem, we compare in detail the cluster structure of various approximate VB and FCI wave functions, since there is only one nonequivalent t_3 amplitude and one t_4 amplitude. However, the approximate VB wave functions violate the alternancy symmetry (since we use OEAOs), so that we have two nonequivalent t_3 (and,

Table 3. FCI correlation energies (in eV) for the PPP π-electron models of *trans*-butadiene (TB) and all-*trans*-hexatriene (ATH) as a function of the resonance integral β (in eV)

$-\beta$ (eV)	$E_{\text{corr}}^{(\text{TB})}$ (eV)	$E_{\text{corr}}^{(\text{ATH})}$ (eV)
0.0	−6.77056	−8.34359
0.1	−5.17229	−7.75625
0.2	−4.80522	−7.20069
0.3	−4.46394	−6.68253
0.4	−4.14931	−6.20393
0.5	−3.86099	−5.76491
0.6	−3.59794	−5.36420
0.7	−3.35862	−4.99967
0.8	−3.14131	−4.66878
0.9	−2.94413	−4.36876
1.0	−2.76525	−4.09681
1.5	−2.08697	−3.06913
2.0	−1.65220	−2.41528
2.4	−1.40899	−2.05214

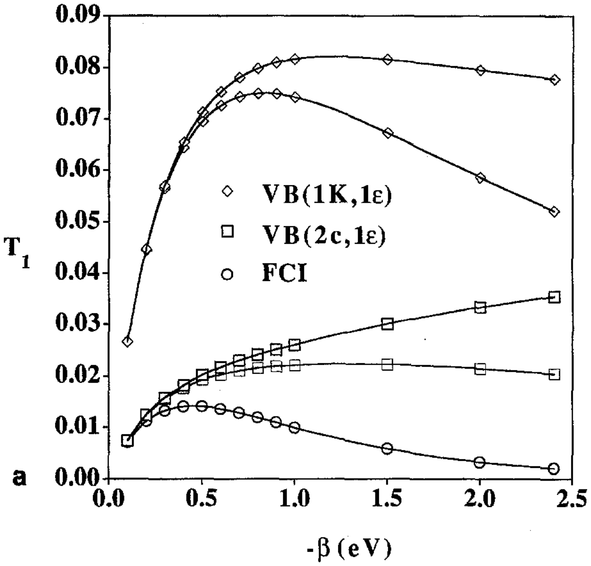

Fig. 11. (Continued)

similarly, t_1) cluster amplitudes. These various amplitudes, resulting from the ($1K$, 1ε) and ($2c$, 1ε) VB wave functions are compared with the corresponding FCI amplitudes in Fig. 11. For the t_1 and t_3 amplitudes, we see that the best approximation is obtained in the fully correlated limit, where each covalent structure represents an exact solution. However, when considering a single Kekulé structure wave function, the t_4 amplitude is very poorly described. In fact, in the $\beta = 0$ limit, this

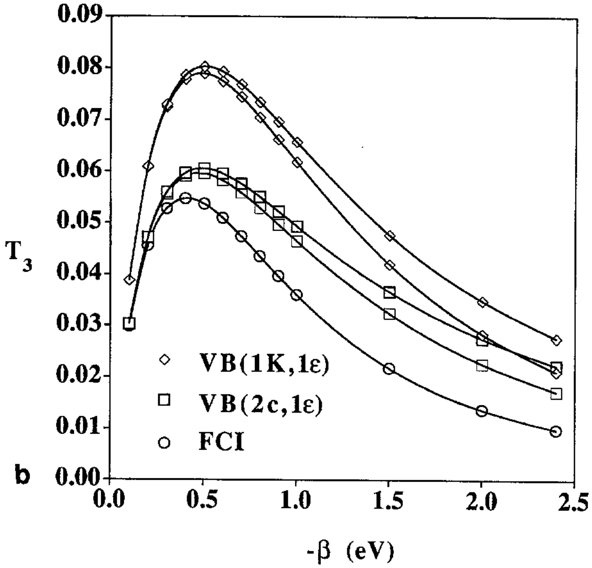

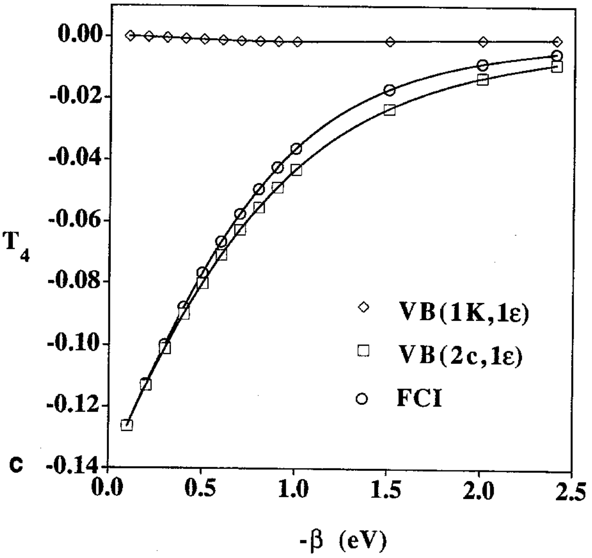

Fig. 11a–c. Dependence of t_1 (**a**), t_3 (**b**) and t_4 (**c**) cluster amplitudes for the *trans*-butadiene π-electron model, resulting from the FCI and two approximate VB wave functions (involving one Kekulé and five covalent structures, respectively), on the resonance integral β (in eV). Note that due to the alternancy symmetry breaking in the PPP-VB models, two distinct t_1 and t_3 amplitudes result (see the text for details)

t_4 amplitude exactly vanishes. Thus, only the T_2 cluster component is present in the Kekulé structure wave function constructed from the orthonormal PPP AOs. On the other hand, the t_4 amplitude originating from the non-Kekulé covalent structure (with bonds between central and terminal carbons) equals -6. The proper zero order eigenstate that corresponds to the ground state $\beta=0$ limit is a linear

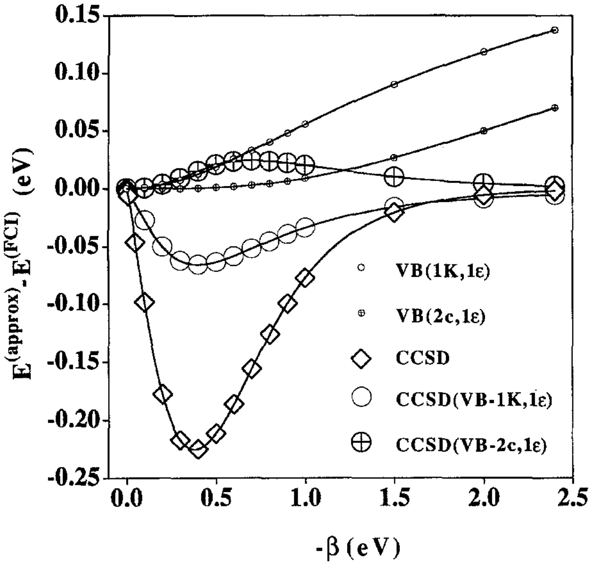

Fig 12. Difference between approximate and FCI correlation energies (in eV) of the π-electron model of *trans*-butadiene as a function of the resonance integral β (in eV), obtained with the PPP-VB, CCSD and CCSD-VB methods

combination of Kekulé and non-Kekulé structures with coefficients $-\sqrt{2/3}$ and $(\sqrt{3}-1)/\sqrt{6}$, respectively (note that the overlap between these structures is $S=\frac{1}{2}$ since in the $\beta=0$ limit we have $\varepsilon_1=0$). This wave function then yields the exact t_4 amplitude in the fully correlated limit as Fig. 11c indicates.

Turning now to the energetic considerations, we compare the correlation energies relative to the FCI result for PPP-VB and CCSD-VB methods, obtained with VB wave functions involving one Kekulé and 2 covalent structures (using only one mixing parameter), as well as for the standard CCSD method (see Fig. 12). We see again that the VB (1*K*, 1ε) and VB (2*c*, 1ε) energies give the exact result in the $\beta=0$ limit aFnd steadily deteriorate with increasing $|\beta|$. On the other hand, CCSD approaches provide a very good approximation in the weakly correlated region and not so good results for highly correlated regime (e.g., $0<|\beta|<2$ eV). In particular, the standard CCSD energies deviate most strongly from the exact result even though in this case all methods recover the exact correlation energy in the $\beta=0$ limit. We see from Fig. 12 that the error arising in the standard CCSD approach is greatly diminished when these equations are corrected for the T_3, T_4 and T_1T_3 clusters.

The fully correlated limit ($\beta=0$) deserves a special attention in this case. As we have already indicated above, we have that $T_1=T_3=T_4=0$ for the Kekulé structure wave function $|\Phi_K\rangle$ in the $\beta=0$ limit (i.e., constructed from the orthonormal PPP AOs), while $T_4\neq 0$ for the non-Kekulé structure $|\Phi_D\rangle$ (we shall refer to it as a Dewar structure by analogy to benzene). Both Kekulé and Dewar structures represent an exact eigenstate of the PPP Hamiltonian when $\beta=0$ [26]. We also know that a proper zero order wave function $|\Phi_0\rangle$ corresponding to the ground state is given by the linear combination $|\Phi_0\rangle=C_K|\Phi_K\rangle+C_D|\Phi_D\rangle$ with $C_K=-\sqrt{2/3}$ and $C_D=(\sqrt{3}-1)/\sqrt{6}$. It is now interesting to consider the CCSD

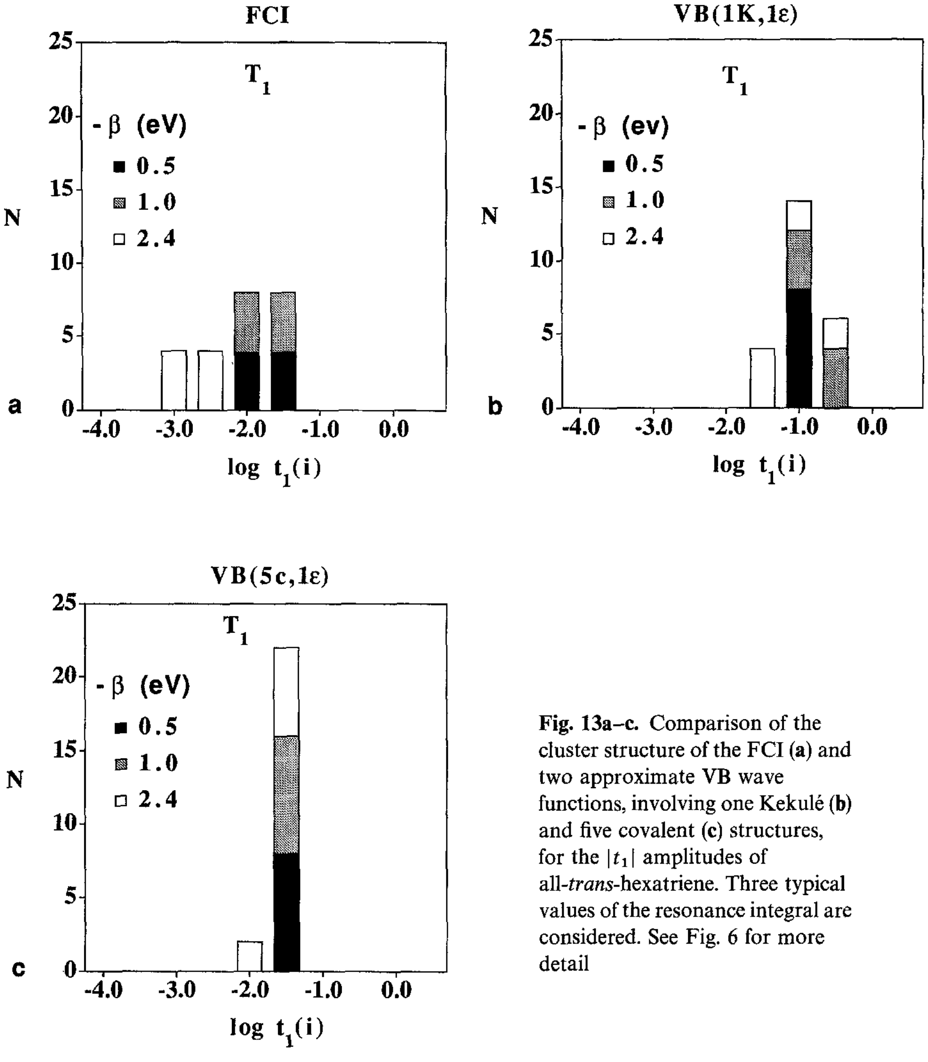

Fig. 13a–c. Comparison of the cluster structure of the FCI (**a**) and two approximate VB wave functions, involving one Kekulé (**b**) and five covalent (**c**) structures, for the $|t_1|$ amplitudes of all-*trans*-hexatriene. Three typical values of the resonance integral are considered. See Fig. 6 for more detail

equations together with the CCSD-VB corrected equations using the cluster components characterizing $|\Phi_K\rangle$, $|\Phi_D\rangle$ and $|\Phi_0\rangle$. In fact, in the case of $|\Phi_K\rangle$, there is no difference between the two sets since $T_1 = T_3 = T_4 = 0$. Using now the t_2 cluster amplitudes associated with these various VB wave functions as the initial guess, we find that while the CCSD solution changes in the first iteration, the CCSD energy does not. However, in the case of the $|\Phi_D\rangle$ and $|\Phi_0\rangle$ corrected CCSD-VB equations, these t_2 cluster amplitudes represent also the solutions of the correspondingly corrected CCSD equations. Of course, the same correlation energy results in each case. We thus see that similarly to the CI case, the degeneracy

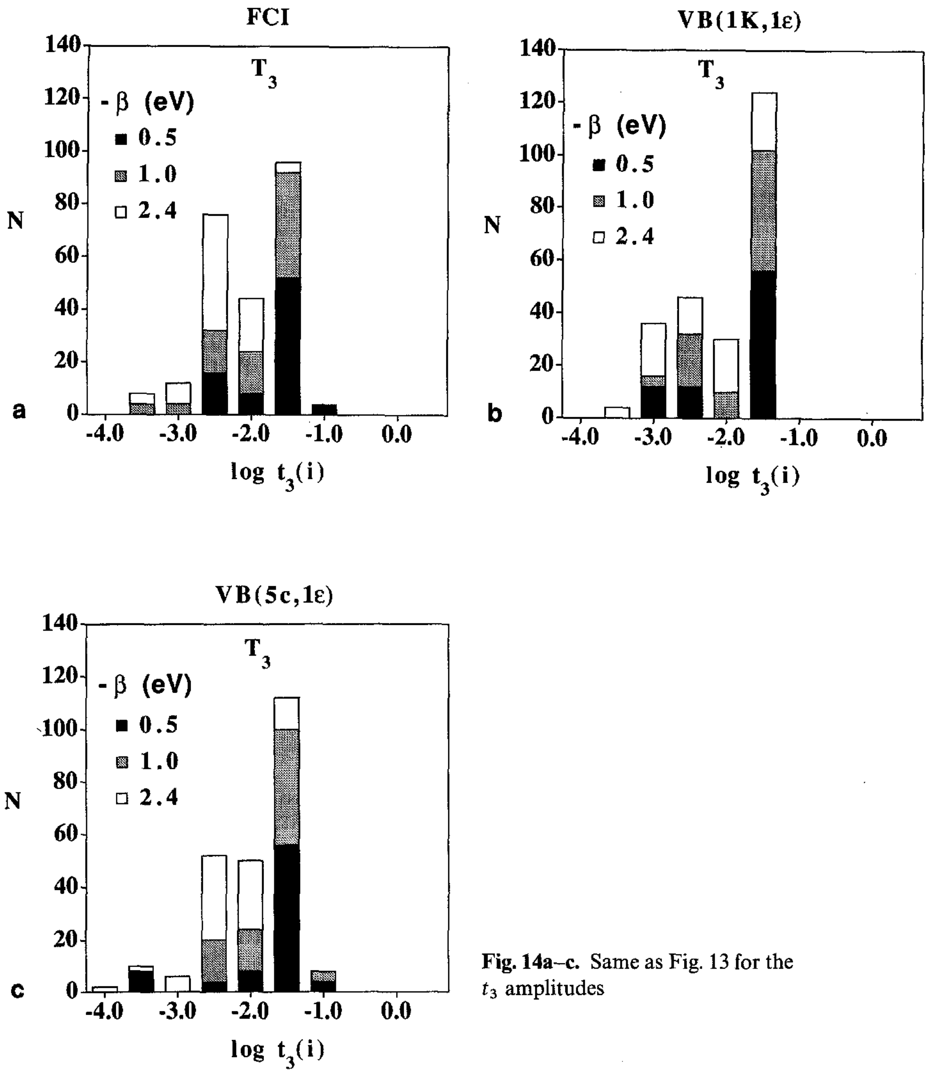

Fig. 14a–c. Same as Fig. 13 for the t_3 amplitudes

characterizing the $\beta = 0$ limit manifests itself in the structure of the solution manifold of the CCSD problem as well (cf., also [27]).

3.2.2 All-trans-hexatriene. A comparison of the cluster structure resulting from the FCI and PPP-VB calculations with one Kekulé or all 5 covalent structures is displayed nomogramatically in Figs. 13–15. We see that both approximate VB wave functions yield rather similar distributions for the T_3 amplitudes, particularly for small $|\beta|$ values, while the T_4 amplitudes are better represented by the VB wave function involving all 5 covalent structures. This may be expected when we realize

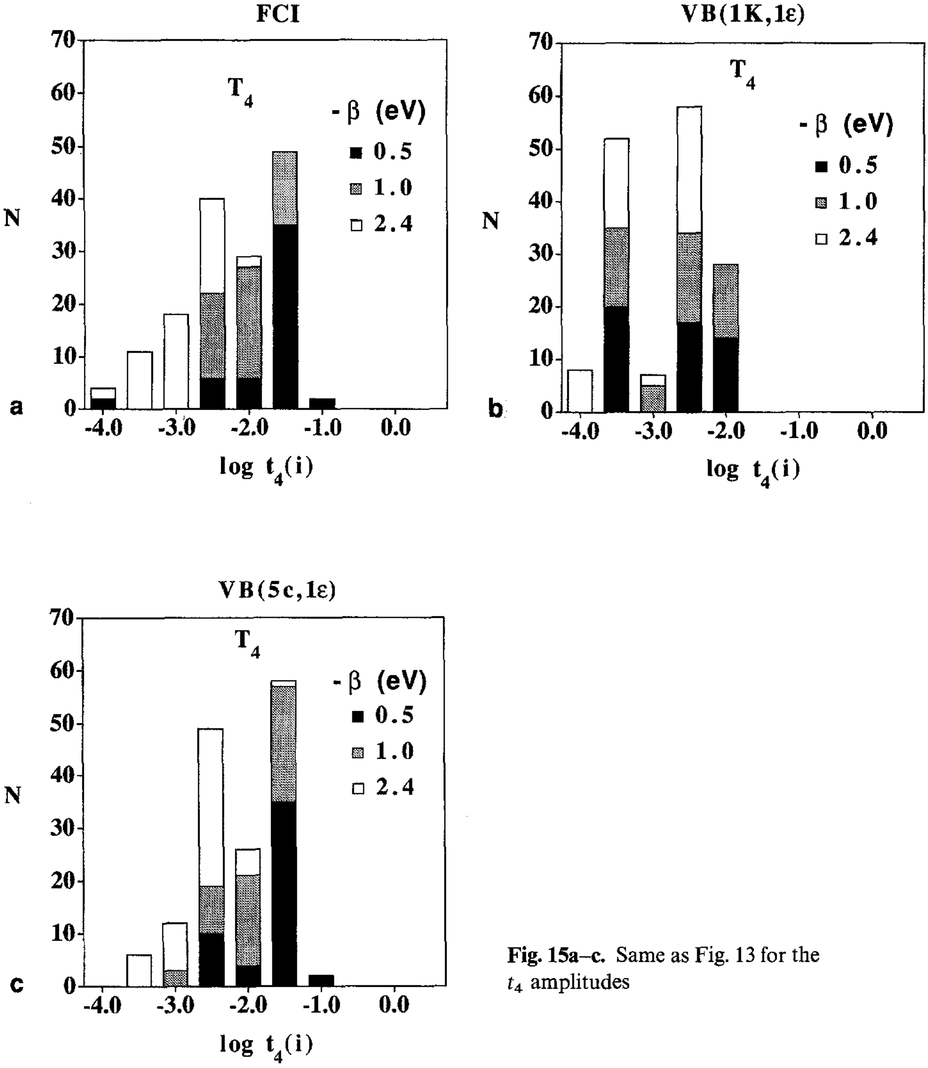

Fig. 15a–c. Same as Fig. 13 for the t_4 amplitudes

that it is exactly the highly correlated limit where the covalent structures play the most important role.

Calculating the correlation energies (cf. Fig. 16) we observe a very similar behavior as in the case of butadiene, except that with the CCSD methods we encounter convergency problems for small $|\beta|$ values and that the deviations from the exact FCI results are much larger. We also see quite distinctly the essential role of other than Kekulé-type covalent structures. Only in this case were we able to obtain converged CCSD-VB solutions in the whole range of $|\beta|$ values, even though the "analytical continuation" procedure from both weakly and fully correlated limits had to be employed, relying on very good estimates of cluster amplitudes used as the starting approximation.

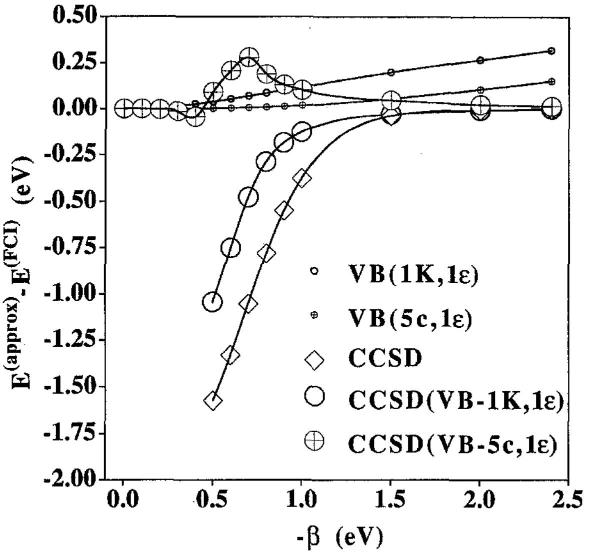

Fig. 16. Same as Fig. 12 for all-*trans*-hexatriene

4 Conclusions

The results presented in this paper clearly demonstrate the potential of using the information about the connected 3- and 4-body clusters, issuing from approximate VB-type wave functions, to correct the standard CCSD equations and thus to extend their utility even in situations where the standard formalism can no longer be employed. We should emphasize in this connection the complementarity of the MO and VB descriptions, particularly when we are interested in a continuous transition between different correlation regimes or in potential energy surfaces involving a dissociation or a bond formation. In this respect the studied models offer an excellent opportunity for testing of these ideas in spite of their obvious limitations. Moreover, these studies offer another insight into the cluster structure of various wave functions and into the role of higher than pair clusters in the CC formalism, particularly when the assumption of the ground state nondegeneracy is being violated.

In the next paper (Part III) of this series, we shall in fact explore some simple models of bond breaking or formation, relying again on the PPP model Hamiltonians. In view of these results it would be certainly desirable to explore this idea at the *ab initio* level, using either the GVB or spin-coupled VB wave functions. In view of the approximate nature of this approach, it would also be worthwhile to explore the possibility of truncating the 3- and 4-body sets of connected cluster amplitudes and their efficient computation. We hope to address these problems in the future.

Acknowledgements. J. Planelles expresses his gratitude to one of his co-authors, Professor J. Paldus, for his hospitality and helpful discussion during his stay in the Department of Applied Mathematics, University of Waterloo. One of us (J. Planelles) wishes to acknowledge the financial support by the Dirección General de Investigacion Científica y Ténica of Spain that enabled him to visit the Department of Applied Mathematics of the University of Waterloo for the academic year 1992–93. The continued support by NSERC (J. Paldus) is also gratefully acknowledged.

References

1. Čížek J (1966) J Chem Phys 45:4256; idem (1969) Adv Chem Phys 14:35; Čížek J, Paldus J (1971) Int J Quantum Chem 5:359; Paldus J, Čížek J , Shavitt I (1972) Phys Rev A5:50
2. For recent reviews, see (a) Bartlett RJ (1989) J Phys Chem 93:1697; (b) Paldus J (1992) In: Wilson S, Diercksen GHF (eds) Methods in computational molecular physics, NATO ASI Series, Series B, Vol. 293. Plenum, New York, p 99; (c) idem (1994) In: Malli GL (ed) Relativistic and correlation effects in molecules and solids, NATO ASI Series B, Vol. 318. Plenum, New York, p 207 and references therein
3. Zhi He, Cremer D (1991) Int J Quantum Chem Symp 25:43; idem (1993) Theor Chim Acta 85:305
4. Jankowski K, Paldus J (1980) Int J Quantum Chem 18:1243; Adams BG, Jankowski K, Paldus J (1981) Phys Rev A 24:2316; idem (1981) ibid 24:2380
5. Paldus J, Takahashi M, Cho RWH (1984) Phys Rev B 30:4267; Paldus J, Boyle MJ (1982) Int J Quantum Chem 22:1281
6. Piecuch P, Zarrabian S, Paldus J, Čížek J (1990) Phys Rev B 42:3351
7. Paldus J, Planelles J (1994) Theor Chim Acta (referred to as Part I)
8. Parr RG (1963) The quantum theory of molecular electronic structure. Benjamin, New York
9. Paldus J (1976) In: Eyring H, Henderson D (eds) Theoretical chemistry: advances and perspectives, Vol 2. Academic, New York, p 131
10. Paldus J (1974) J Chem Phys 61:5321
11. Li X, Paldus J (1991) J Mol Struct (Theochem) 229:249
12. Li X, Paldus J (1992) Int J Quantum Chem 41:117
13. Mulliken RS (1949) J Chim Phys 46:497; for English translation see: idem (1975) In: Ramsay DA, Hinze J (eds) Selected papers of Robert S. Mulliken. University of Chicago Press, Chicago, p 899; idem (1962) J Phys Chem 56:295; see also the Appendix of the paper by Koutecký J, Paldus J (1962) Coll Czech Chem Commun 27:599
14. Paldus J, Chin E (1983) Int J Quantum Chem 24:373; Takahashi M, Paldus J (1985) ibid 28:459 and references therein
15. Planelles J, Paldus J, Li X (1994) Theor Chim Acta (Part III)
16. Mataga N, Nishimoto K (1957) Z Phys Chem 13:140
17. Gerratt J, Raimondi M (1980) Proc Roy Soc (London) A 371:525
18. McWeeny R (1988) Int J Quantum Chem 34:25
19. Paldus J, Li X (1991) Israel J Chem 31:351
20 Paldus J, Li X (1992) In: Frank A, Seligman TH, Wolf KB (eds) Group theory in physics, AIP conference proceedings 266. American Institute of Physics, New York, p 159
21. (a) Paldus J, Sarma CR (1985) J Chem Phys 83:5135; (b) Paldus J, Gao MJ, Chen JQ (1987) Phys Rev A 35:3197; (c) Paldus J, Jeziorski B (1988) Theor Chim Acta 73:81; (d) Paldus J, Rettrup S, Sarma CR (1989) J Mol Struct (Theochem) 199:85
22. Paldus J (1988) In: Truhlar DG (ed) Mathematical frontiers in computational chemical physics, IMA Series, Vol. 15. Springer, Berlin, p 262
23. Li X, Zhang Q (1989) Int J Quantum Chem 36:599; Zhang Q, Li X (1989) J Mol Struct (Theochem) 198:413
24. Waller I, Hartree RD (1929) Proc Roy Soc (London) A 124:119
25. Kucharski SA, Balková A, Bartlett RJ (1991) Theor Chim Acta 80:321
26. Čížek J, Paldus J, Hubač I (1974) Int J Quantum Chem 8:951
27. Piecuch P, Paldus J (1991) Int J Quantum Chem Symp 25:9